Qiong-Yao Zhan, Di-Cheng Zhu, Qing Wang, Peter A. Cawood, Jin-Cheng Xie, Xiang Liu, Shi-Min Li, Liang-Liang Zhang, and Zhi-Dan Zhao, 2021, Imaging the Late Triassic lithospheric architecture of the Yidun Terrane, eastern Tibetan Plateau: Observations and interpretations: GSA Bulletin, https://doi.org/10.1130/B35778.1.

Supplemental Material

1. Analytical Methods

1.1. LA-ICP-MS zircon U-Pb dating

Zircons were separated from pulverized rock by conventional heavy liquid and magnetic techniques at the Lab of Geological Team of Hebei Province, China. Separated zircon grains from each sample were mounted in epoxy resin and polished to expose their interior. Cathodoluminescence (CL) images were obtained at the Institute of Geology, Chinese Academy of Geological Sciences (Beijing) to select suitable positions for in situ analysis. In situ U-Th-Pb isotopes of zircons were measured by LA-ICP-MS using an Agilent 7900 ICP-MS system attached to a NewWave 193 nm excimer ArF laser-ablation system at the Milma Lab of China University of Geosciences (Beijing). All spot analyses were carried out using a beam diameter of 35 μm with a repetition rate of 10 Hz and laser uence of 4–8 J/cm^2. Each spot analysis incorporated a background acquisition of ~20 s (gas blank), 50 s data acquisition, and 30 s delay to wash out the previous sample and prepare the next analysis. Zircon 91500 (Wiedenbeck et al., 1995) was used as external standard to calibrate U-Pb dating. The Plešovice zircon (Sláma et al., 2008) and zircon GJ-1 (Jackson et al., 2004) were treated as unknown and used to check the reproducibility and accuracy of the calibration. In each cycle, every six spot analyses were followed by analyzing zircon 91500 twice and one Plešovice and one GJ-1 (i.e., 2 zircon 91500 + 1 Plešovice + 1 GJ-1 + 6 sample spots + 2 zircon 91500 + 1 Plešovice + 1 GJ-1). Off-line data conduction was performed using an Excel-based software ICPMSDataCal (Liu et al., 2010). Concordia diagrams and weighted mean calculations were made using Isoplot/Ex_ver3 (Ludwig, 2003).

1.2. In Situ Zircon Hf Isotope Measurements

In situ zircon Hf isotope measurements were conducted at the Institute of Geology and Geophysics, Chinese Academy of Sciences by using a Neptune multi-collector (MC)-ICP-MS with an attached 193 nm excimer ArF laser-ablation system. Lu-Hf isotope analyses were made on the same zircon grains previously analyzed for U–Pb isotopes. During analysis, a laser repetition rate of 4 Hz was used with spot sizes of 20 or 60 μm depending on zircon grain size. Raw count rates for ^{172}Yb, ^{173}Yb, ^{175}Lu, ^{176}(Hf+Yb+Lu), ^{177}Hf, ^{178}Hf, ^{179}Hf, ^{180}Hf and ^{182}W were collected during analysis. The detailed analytical procedure was described by Wu et al. (2006). Zircon 91500 and Mud Tank were used as external standards and were analyzed once and twice, respectively before and after every 10 analyses. Initial ^{176}Hf/^{177}Hf ratios were calculated by using the ^{176}Lu decay constant of 1.867×10^{-11} yr^{-1} (Söderlund et al., 2004) and measured ^{176}Lu/^{177}Hf. Chondrite Lu-Hf isotopic values (^{176}Lu/^{177}Hf = 0.0336 and ^{176}Hf/^{177}Hf = 0.282785) reported by Bouvier et al. (2008) are used to calculate $\varepsilon_{Hf}(t)$ values.

1.3. Whole-rock Major and Trace Element Analysis

Major element oxides (wt.%) were measured on fused glass discs, using an X-ray fluorescence (Axios MAX) at the Wuhan SampleSolution Analytical Technology Co., Ltd., Wuhan, China (WSSATCL). Three USGS rock standards (BHVO-2, W-2a, and GSP-2) and two Chinese national rock standards (GBW07103 and GBW07316) were used for calibration. The

analytical uncertainties are generally better than 5% for all elements. Loss on ignition (LOI) was obtained by twice heating.

Whole-rock trace elements were measured by Agilent 7700e ICP-MS at the WSSATCL. Sample powder (200 mesh) were firstly dried for 12 h in an oven at 105 °C. Then 50 mg accurately weighed power was placed in a Teflon bomb followed by slowly adding in 1 ml HNO_3 and 1 ml HF. The Teflon bomb was putted in a stainless steel pressure jacket and heated to 190 °C in an oven for more than 24 h. After cooling, the Teflon bomb was opened and evaporated to incipient dryness on a 140 °C hotplate. Then 1 ml HNO_3 was added in and it was evaporated to dryness again. After evaporation, 1 ml of HNO_3, 1 ml of MQ water, and 1 ml In solution (1 ppm) used as internal standard were added and the Teflon bomb was resealed and placed in the oven for more than12 h heating at 190 °C. At last, the final solution was diluted to 100 g in a polyethylene bottle by the addition of 2% HNO_3. Four USGS rock standards (AGV-2, BHVO-2, BCR-2, and RGM-2) were used to calibrate the elemental concentrations of samples.

2. LA-ICP-MS ZIRCON U-Pb DATING RESULTS

Nine samples were selected for LA-ICP-MS zircon U-Pb dating. The dating results are reported in Table S1 and illustrated on a concordia and weighted mean age diagram (Fig. S1). All dated samples yielded Late Triassic ages ranging from ~212 Ma to ~220 Ma. Within sample variations of zircon ages are large for most dated samples indicated by large MSWD values. The large MSWD value may indicate that the uncertainty of individual zircon age is underestimated or it may suggest that more than one age population exist, for example, antecrysts recycled from previous batches of magmatism. A thorough work on this issue is beyond the scope of this study and will be covered in a separate study. Currently, a weighted mean $^{206}Pb/^{238}U$ age is calculated for each sample from all concordant ages which form a continuous trend in $^{206}Pb/^{238}U$ age distribution diagram. However, ages obviously away from the continuous trend are not included in calculation of the weighted mean age.

3. DATA SETS AND FIGURES

Tables S1–S7 are listed in an Excel file

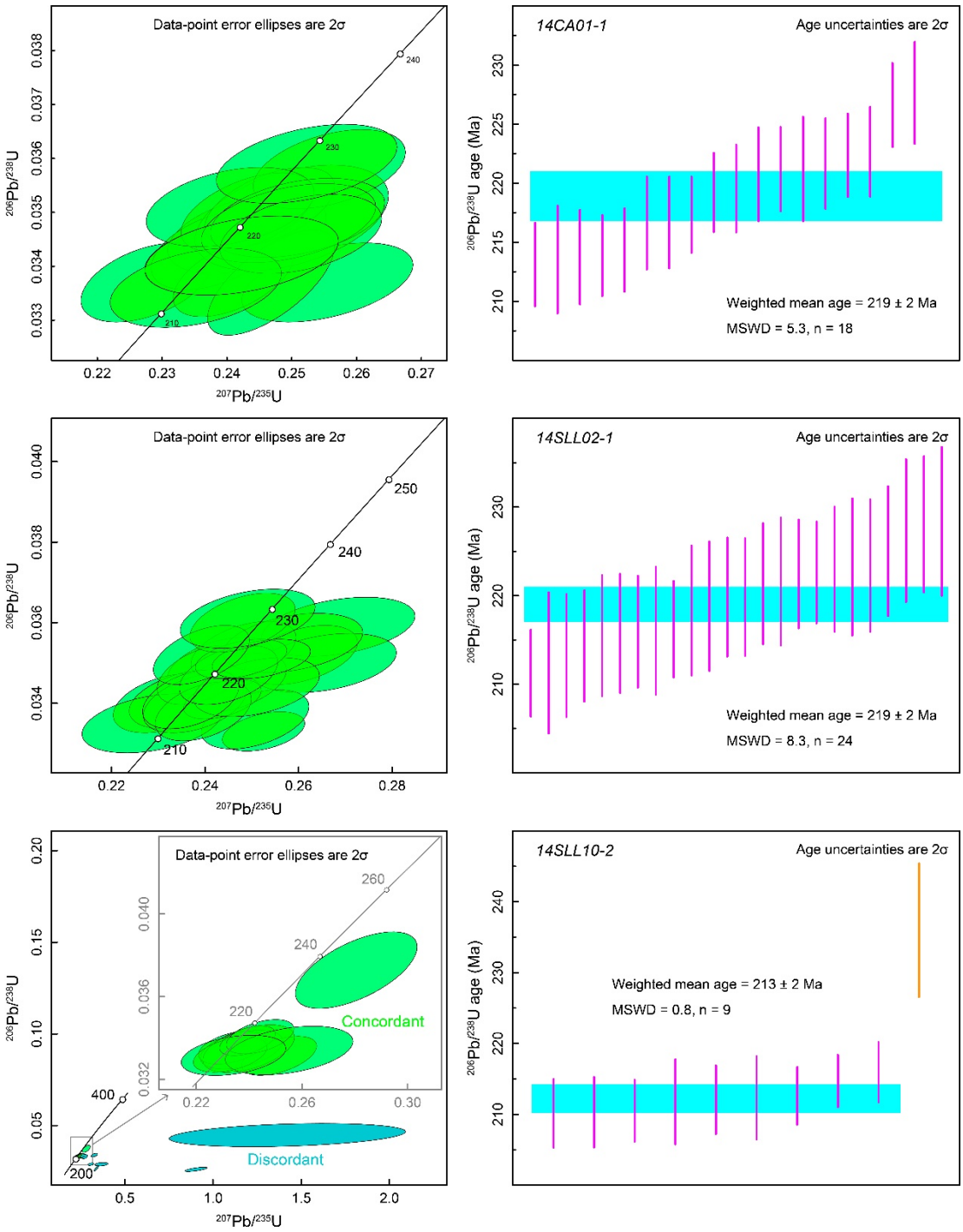

Figure S1. Zircon U-Pb concordia and weighted mean age diagram of nine samples from Late Triassic plutons in the Yidun Terrane, eastern Tibetan Plateau. Green ellipses represent concordant results with 90% to 110% concordance and blue ellipses represent discordant results. Weighted mean age with 2σ uncertainty is represented by light blue box and is calculated from concordant ages which form a continuous trend (pink lines) in the $^{206}Pb/^{238}U$ age distribution. Ages away from the continuous trend (brown lines) are not included in the calculation of the mean age.

Figure S1. *Continued.*

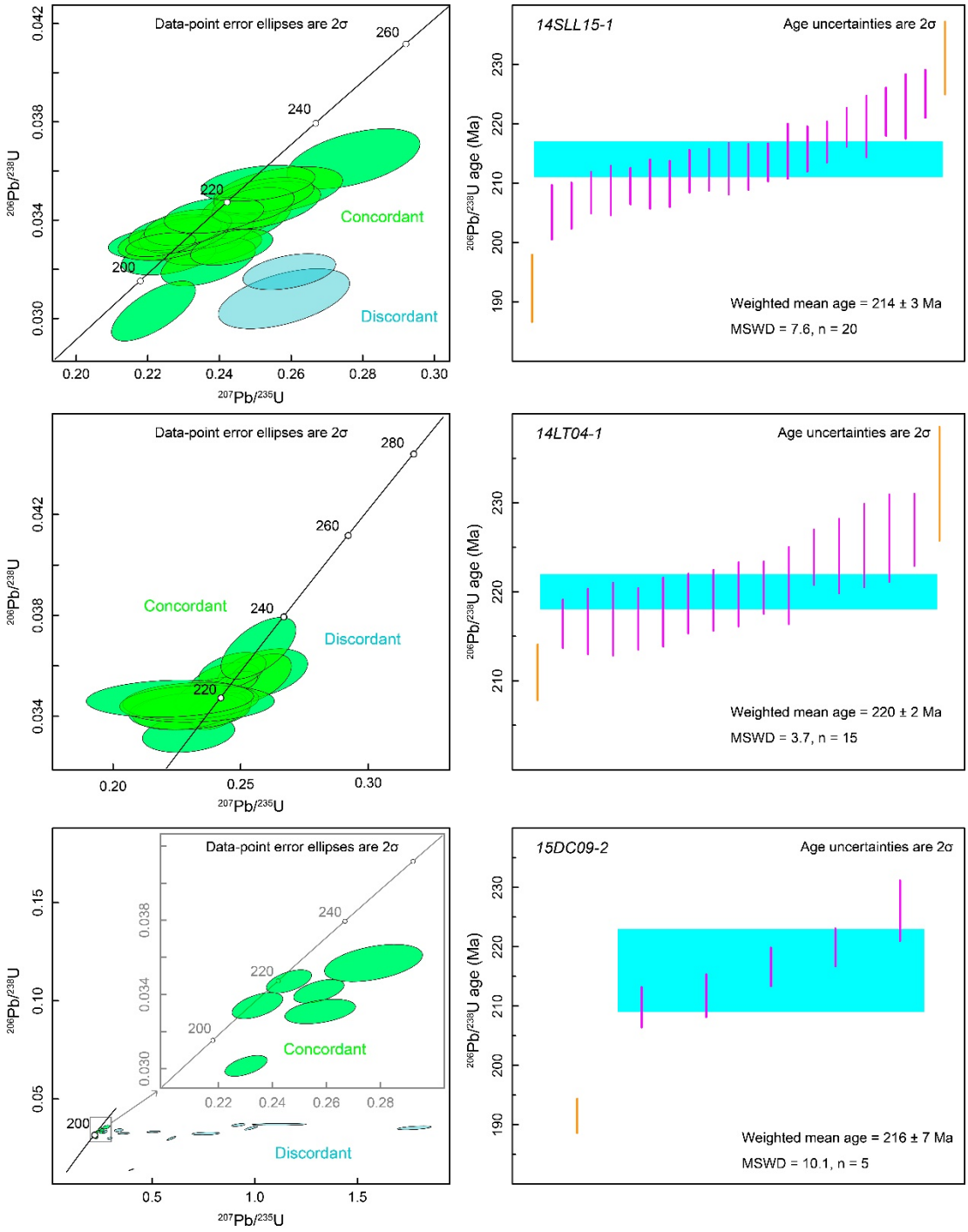

Figure S1. *Continued.*

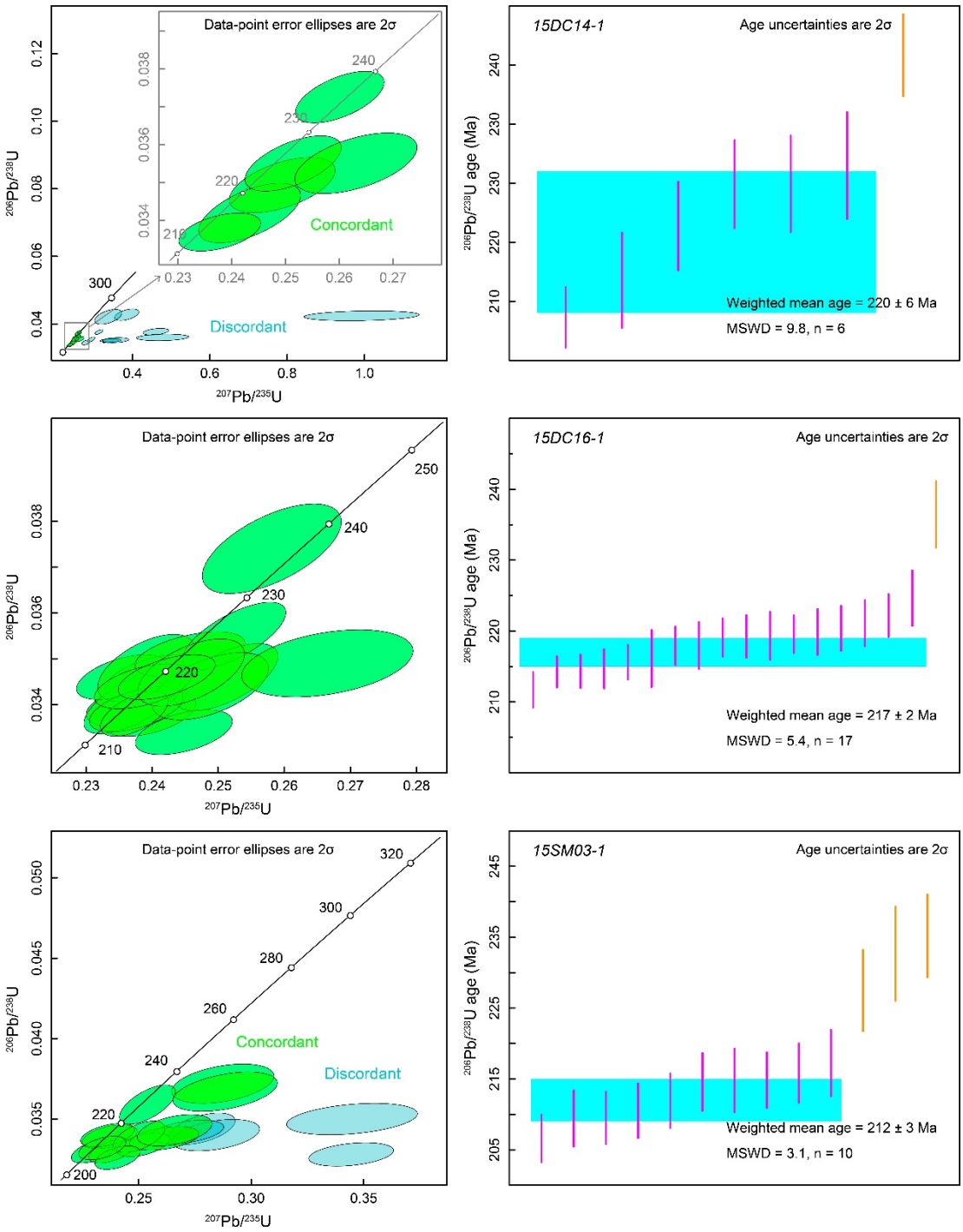

Figure S1. *Continued.*

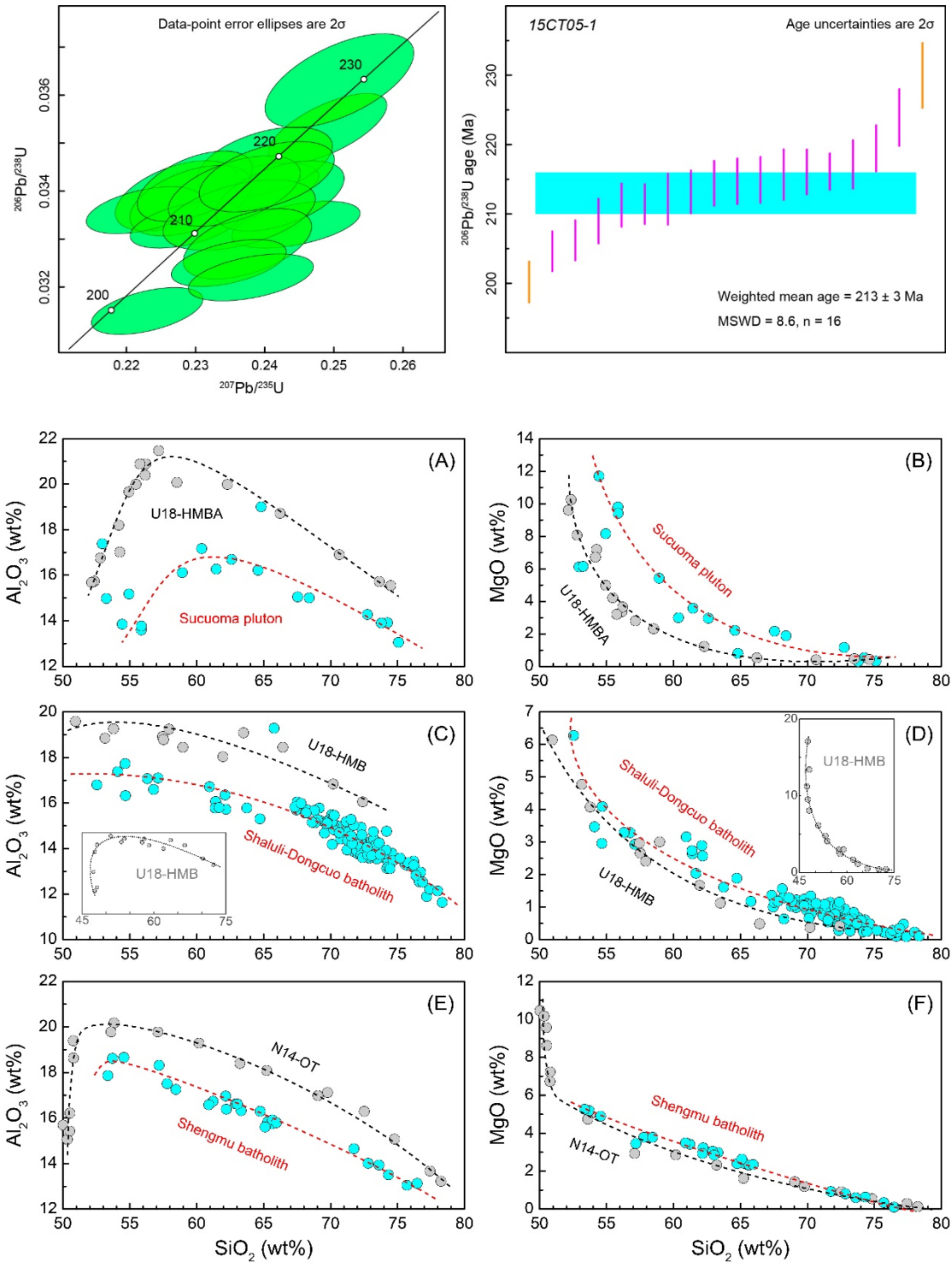

Figure S2. Whole-rock Al_2O_3 and MgO versus SiO_2 contents of samples from the Sucuoma pluton (A, B), Shaluli-Dongcuo batholith (C, D), and Shengmu batholith (E, F) in the Yidun Terrane. Red dashed lines depict the interpreted liquid line of descend (LLD) of the above plutons. Black dashed lines are LLD of hydrous fractional crystallization of a high-Mg basaltic andesite (U18-HMBA) at 1.0 GPa (Ulmer et al., 2018), a high-Mg basalt (U18-HMB) at 1.0 GPa

(Ulmer et al., 2018), and an olivine tholeiite (N14-OT) at 0.7 GPa (Nandedkar et al., 2014). Only part of the LLD of U18-HMB is shown in C and D due to space limitation and the insets in C and d show the intact LLD of U18-HMB. The LLD in these experiments are shown here to reveal that fractional crystallization of mantle derived primitive magmas producing intermediate to silicic magmas will result in curvatures in certain major element systematics. The position of kinks of the LLD is not fixed at given SiO_2 and is related to the composition of parental magmas, crystallization pressure and temperature, and fractionation assemblages. Note that the LLD of N14-OT at the part of SiO_2 > 52 wt% is nearly a straight line. See text for discussion.

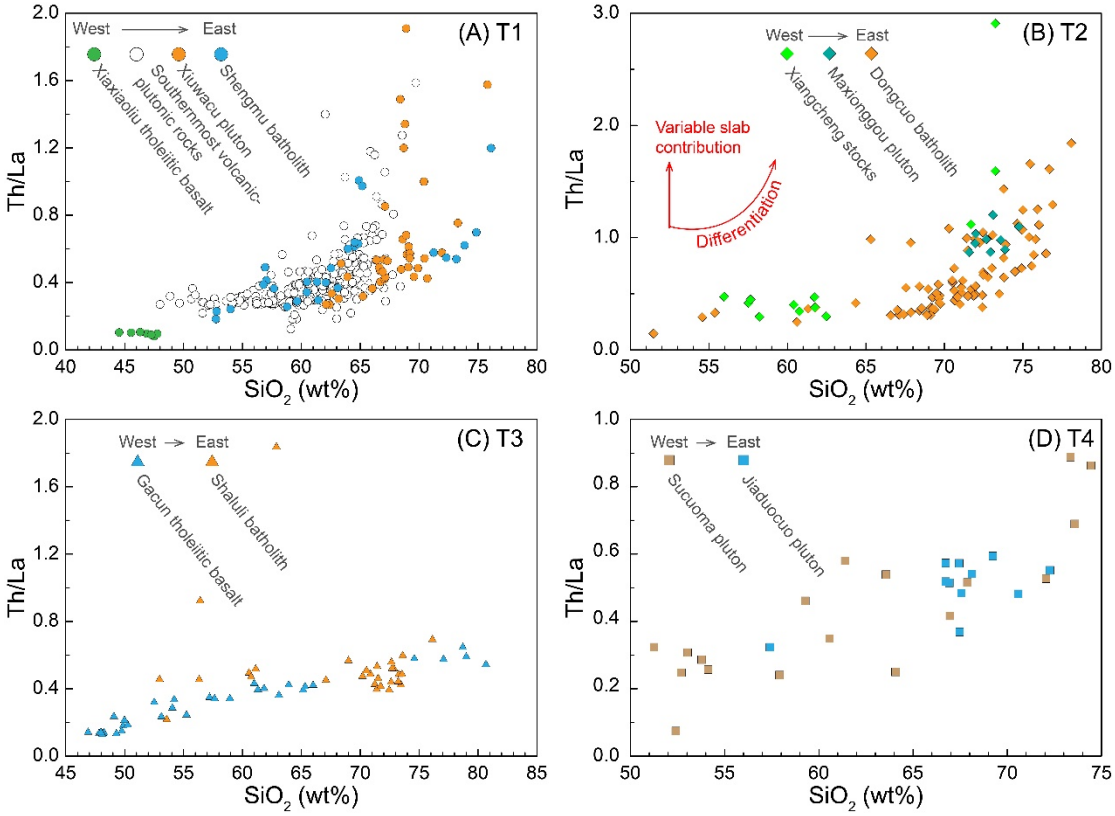

Figure S3. Th/La versus SiO_2 diagram for Late Triassic magmatic rocks along four transects (T1–T4) across the Yidun Terrane. See Figure 1 in the text for locations of the four transects. The Th/La ratio of mafic rocks is a proxy for subduction slab contribution to mantle source (Plank, 2005). Note that mafic rocks derived from variably enriched mantle sources will show different Th/La ratios at given SiO_2 content and manga crystallization differentiation will result in increase of Th/La ratios with increase of SiO_2 (see the different trends depicted in B). From west to east in each transect, mafic rocks show relatively constant rather than increase in Th/La ratios, indicating that west to east enriched in isotopic compositions did not result from higher degree of subduction-related alteration of the lithospheric mantle in the east. See text for discussions.

REFERENCES CITED (including references cited in Tables S4–S7)

Bouvier, A., Vervoort, J.D., and Patchett, P.J., 2008, The Lu–Hf and Sm–Nd isotopic composition of CHUR: Constraints from unequilibrated chondrites and implications for the bulk composition of terrestrial planets: Earth and Planetary Science Letters, v. 273, p. 48–57, https://doi.org/10.1016/j.epsl.2008.06.010.

Cao, K., Xu, J.-F., Chen, J.-L., Huang, X.-X., Ren, J.-B., Zhao, X.-D., and Liu, Z.-X., 2016, Double-layer structure of the crust beneath the Zhongdian arc, SW China: U–Pb geochronology and Hf isotope evidence: Journal of Asian Earth Sciences, v. 115, p. 455–467, https://doi.org/10.1016/j.jseaes.2015.10.024.

Cao, K., Yang, Z.-M., Xu, J.-F., Fu, B., Li, W.-K., and Sun, M.-Y., 2018, Origin of dioritic magma and its contribution to porphyry Cu–Au mineralization at Pulang in the Yidun arc, eastern Tibet: Lithos, v. 304–307, p. 436–449, https://doi.org/10.1016/j.lithos.2018.02.018.

Chen, J.-L., Xu, J.-F., Ren, J.-B., Huang, X.-X., and Wang, B.-D., 2014, Geochronology and geochemical characteristics of Late Triassic porphyritic rocks from the Zhongdian arc, eastern Tibet, and their tectonic and metallogenic implications: Gondwana Research, v. 26, p. 492–504, https://doi.org/10.1016/j.gr.2013.07.022.

Chen, J., Xu, J., Ren, J., and Huang, X., 2017, Late Triassic E-MORB-like basalts associated with porphyry Cu-deposits in the southern Yidun continental arc, eastern Tibet: evidence of slab-tear during subduction?: Ore Geology Reviews, v. 90, p. 1,054–1,062, https://doi.org/10.1016/j.oregeorev.2016.12.006.

Fang, X., 2017, Petrogenesis of the Middle-Late Triassic intermediate-acid intrusive rocks in the Yidun terrane and its geological significances [Master thesis]: Beijing, University of Chinese Academy of Sciences, 117 p.

Gao, X., Yang, L.Q., Zhang, R.G., and Meng, J.Y., 2019, Nature and origin of Mesozoic granitoids and associated mineralization in the Sanjiang Tethys Orogeny, SW China: the Xiuwacu complex example: International Geology Review, v. 61, p. 795–820, https://doi.org/10.1080/00206814.2018.1464405.

Han, Z., 2018, Basalt characteristics and tectonic significance in the southern of Garze-Litang suture zone [M.S. thesis]: Mianyang, Southwest University of Science and Technology, 86 p.

He, D.-F., Zhu, W.-G., Zhong, H., Ren, T., Bai, Z.-J., and Fan, H.-P., 2013, Zircon U–Pb geochronology and elemental and Sr–Nd–Hf isotopic geochemistry of the Daocheng granitic pluton from the Yidun Arc, SW China: Journal of Asian Earth Sciences, v. 67–68, p. 1–17, https://doi.org/10.1016/j.jseaes.2013.02.002.

Jackson, S.E., Pearson, N.J., Griffin, W.L., and Belousova, E.A., 2004, The application of laser ablation-inductively coupled plasma-mass spectrometry to in situ U–Pb zircon geochronology: Chemical Geology, v. 211, p. 47–69, https://doi.org/10.1016/j.chemgeo.2004.06.017.

Jiang, L., Xue, C., Hou, Z., and Xiang, K., 2015, Petrogenesis of the Bengge syenites, northwestern Yunnan: Geochemistry, geochronology and Hf isotopes evidence: Acta Petrologica Sinica, v. 31, p. 3234–3246.

Kong, D.-X., Xu, J.-F., and Chen, J.-L., 2016, Oxygen isotope and trace element geochemistry of zircons from porphyry copper system: Implications for Late Triassic metallogenesis within the Yidun Terrane, southeastern Tibetan Plateau: Chemical Geology, v. 441, p. 148–161, https://doi.org/10.1016/j.chemgeo.2016.08.012.

Leng, C.-B., Gao, J.-F., Chen, W.T., Zhang, X.-C., Tian, Z.-D., and Guo, J.-H., 2018, Platinum-group elements, zircon Hf-O isotopes, and mineralogical constraints on magmatic evolution of the Pulang porphyry Cu-Au system, SW China: Gondwana Research, v. 62, p. 163–177, https://doi.org/10.1016/j.gr.2018.03.001.

Leng, C.-B., Huang, Q.-Y., Zhang, X.-C., Wang, S.-X., Zhong, H., Hu, R.-Z., Bi, X.-W., Zhu, J.-J., and Wang, X.-S., 2014, Petrogenesis of the Late Triassic volcanic rocks in the Southern Yidun arc, SW China: Constraints from the geochronology, geochemistry, and Sr–Nd–Pb–Hf isotopes: Lithos, v. 190–191, p. 363–382, https://doi.org/10.1016/j.lithos.2013.12.018.

Leng, C.-B., Zhang, X.-C., Hu, R.-Z., Wang, S.-X., Zhong, H., Wang, W.-Q., and Bi, X.-W., 2012, Zircon U–Pb and molybdenite Re–Os geochronology and Sr–Nd–Pb–Hf isotopic constraints on the genesis of the Xuejiping porphyry copper deposit in Zhongdian, Northwest Yunnan, China: Journal of Asian Earth Sciences, v. 60, p. 31–48, https://doi.org/10.1016/j.jseaes.2012.07.019.

Liu, S., Wang, Z., Yan, Q., Li, Q., Zhang, D., Wang, J., Yang, B., Gu, L., and Zhao, F., 2006, Indosinian tectonic setting of the southern Yidun Arc: Constraints from SHRIMP zircon chronology and geochemistry of dioritic porphyries and granites: Acta Geologica Sinica, v. 80, p. 387–399, https://doi.org/10.1111/j.1755-6724.2006.tb00256.x.

Liu, Y.S., Hu, Z.C., Zong, K.Q., Gao, C.G., Gao, S., Xu, J., and Chen, H.H., 2010, Reappraisement and refinement of zircon U-Pb isotope and trace element analyses by LA-ICP-MS: Chinese Science Bulletin, v. 55, p. 1535–1546, https://doi.org/10.1007/s11434-010-3052-4.

Ludwig, K.R., 2003, ISOPLOT 3.00: A geochronological toolkit for Microsoft Excel, Berkeley, CA, Berkeley Geochronology Center.

McDonough, W.F., and Sun, S.S., 1995, The composition of the Earth: Chemical Geology, v. 120, p. 223–253, https://doi.org/10.1016/0009-2541(94)00140-4.

Mo, X., et al., 1993, Sanjiang Tethys volcanism and related mineralization, Beijing, Geological Publishing House: 267 p.

Nandedkar, R.H., Ulmer, P., and Müntener, O., 2014, Fractional crystallization of primitive, hydrous arc magmas: an experimental study at 0.7 GPa: Contributions to Mineralogy and Petrology, v. 167, p. 1015, https://doi.org/10.1007/s00410-014-1015-5.

Nie, F., 2019, Tectonic evolution and typical deposits in the southern segment of the Ganzi-Litang orogenic belt [Ph.D. thesis]: Beijing, China University of Geosciences, 135 p.

Peng, T., Zhao, G., Fan, W., Peng, B., and Mao, Y., 2014, Zircon geochronology and Hf isotopes of Mesozoic intrusive rocks from the Yidun terrane, Eastern Tibetan Plateau: Petrogenesis and their bearings with Cu mineralization: Journal of Asian Earth Sciences, v. 80, p. 18–33, https://doi.org/10.1016/j.jseaes.2013.10.028.

Plank, T., 2005, Constraints from Thorium/Lanthanum on Sediment Recycling at Subduction Zones and the Evolution of the Continents: Journal of Petrology, v. 46, p. 921–944, https://doi.org/10.1093/petrology/egi005.

Sláma, J., et al., 2008, Plešovice zircon-A new natural reference material for U–Pb and Hf isotopic microanalysis: Chemical Geology, v. 249, p. 1–35, https://doi.org/10.1016/j.chemgeo.2007.11.005.

Söderlund, U., Patchett, P.J., Vervoort, J.D., and Isachsen, C.E., 2004, The 176Lu decay constant determined by Lu–Hf and U–Pb isotope systematics of Precambrian mafic intrusions: Earth and Planetary Science Letters, v. 219, p. 311–324, https://doi.org/10.1016/S0012-821X(04)00012-3.

Ulmer, P., Kaegi, R., and Müntener, O., 2018, Experimentally derived intermediate to silica-rich arc magmas by fractional and equilibrium crystallization at 1.0 GPa: An evaluation of phase relationships, compositions, liquid lines of descent and oxygen fugacity: Journal of Petrology, v. 59, p. 11–58, https://doi.org/10.1093/petrology/egy017.
Vermeesch, P., 2012, On the visualisation of detrital age distributions: Chemical Geology, v. 312–313, p. 190–194, https://doi.org/10.1016/j.chemgeo.2012.04.021.
Wang, B.-Q., Wang, W., and Zhou, M.-F., 2013a, Provenance and tectonic setting of the Triassic Yidun Group, the Yidun Terrane, Tibet: Geoscience Frontiers, v. 4, p. 765–777, https://doi.org/10.1016/j.gsf.2013.02.007.
Wang, B.-Q., Zhou, M.-F., Chen, W.T., Gao, J.-F., and Yan, D.-P., 2013b, Petrogenesis and tectonic implications of the Triassic volcanic rocks in the northern Yidun Terrane, Eastern Tibet: Lithos, v. 175–176, p. 285–301, https://doi.org/10.1016/j.lithos.2013.05.013.
Wang, B.-Q., Zhou, M.-F., Li, J.-W., and Yan, D.-P., 2011, Late Triassic porphyritic intrusions and associated volcanic rocks from the Shangri-La region, Yidun terrane, Eastern Tibetan Plateau: Adakitic magmatism and porphyry copper mineralization: Lithos, v. 127, p. 24–38, https://doi.org/10.1016/j.lithos.2011.07.028.
Wang, P., Dong, G.-C., Zhao, G.-C., Han, Y.-G., and Li, Y.-P., 2018, Petrogenesis of the Pulang porphyry complex, southwestern China: Implications for porphyry copper metallogenesis and subduction of the Paleo-Tethys Oceanic lithosphere: Lithos, v. 304–307, p. 280–297, https://doi.org/10.1016/j.lithos.2018.02.009.
Wang, X.-S., Bi, X.-W., Chen, Y.-W., Pan, L.-C., and Xu, L.-L., 2019, Crystal fractionation of contaminated melts and re-melting of newly underplated basaltic crust generated late Triassic andesitic and dioritic intrusions in the southern Yidun Terrane, SW China: Lithos, v. 342–343, p. 135–151, https://doi.org/10.1016/j.lithos.2019.05.033.
Wiedenbeck, M., Alle, P., Corfu, F., Griffin, W.L., Meier, M., Oberli, F.V., Von Quadt, A., Roddick, J.C., and Spiegel, W., 1995, Three natural zircon standards for U-Th-Pb, Lu-Hf, trace element and REE analyses: Geostandards and Geoanalytical Research: Geostandards and Geoanalytical Research, v. 19, p. 1–23, https://doi.org/10.1111/j.1751-908X.1995.tb00147.x.
Wu, F.-Y., Yang, Y.-H., Xie, L.-W., Yang, J.-H., and Xu, P., 2006, Hf isotopic compositions of thestandard zircons in U-Pb geochronology: Chemical Geology, v. 234, p. 105–126, https://doi.org/10.1016/j.chemgeo.2006.05.003.
Wu, T., 2015, Early Mesozoic magmatism and tectonic evolution of Yidun arc belt, eastern Tibet Plateau [Ph.D. thesis]: Wuhan, China University of Geosciences, 153 p.
Wu, T., Xiao, L., Wilde, S.A., Ma, C.-Q., Li, Z.-L., Sun, Y., and Zhan, Q.-Y., 2016, Zircon U–Pb age and Sr–Nd–Hf isotope geochemistry of the Ganluogou dioritic complex in the northern Triassic Yidun arc belt, eastern Tibetan Plateau: Implications for the closure of the Garzê-Litang Ocean: Lithos, v. 248–251, p. 94–108, https://doi.org/10.1016/j.lithos.2015.12.029.
Wu, T., Xiao, L., Wilde, S.A., Ma, C.-Q., and Zhou, J.-X., 2017, A mixed source for the Late Triassic Garzê-Daocheng granitic belt and its implications for the tectonic evolution of the Yidun arc belt, eastern Tibetan Plateau: Lithos, v. 288–289, p. 214–230, https://doi.org/10.1016/j.lithos.2017.07.002.
Yan, Q., et al., 2005, Opening of the Tethys in southwest China and its significance to the breakup of East Gondwanaland in late Paleozoic: Evidence from SHRIMP U-Pb zircon

analyses for the Garzê ophiolite block: Chinese Science Bulletin, v. 50, p. 256–264, https://doi.org/10.1007/BF02897536.
Yan, S., Duan, Y., Tan, C., and Wen, L., 2019, Identification of the Middle Triassic ocean island rock association in the Garze-Litang ophiolite mélange zone and its tectonic significance: constraints from petrology, geochemistry and geochronology: Acta Geoscientica Sinica, v. 40, p. 816–826.
Yan, T.T., Zhang, X.F., Wang, D., and Yang, Z., 2019, Geochronology, mineralogy, and geochemistry of the Late Triassic Xiuwacu biotite granite in the southern Yidun Terrane, southwest China: Insights into the petrogenesis and magmatic fertility: Geological Journal, https://doi.org/10.1002/gj.3448.
Yang, L.-Q., He, W.-Y., Gao, X., Xie, S.-X., and Yang, Z., 2018, Mesozoic multiple magmatism and porphyry–skarn Cu–polymetallic systems of the Yidun Terrane, Eastern Tethys: Implications for subduction-and transtension-related metallogeny: Gondwana Research, v. 62, p. 144–162, https://doi.org/10.1016/j.gr.2018.02.009.
Zhang, W., Sun, C., Dai, Z., Lei, T., and Xu, S., 2012, A study on the ophiolite along Tongxiao-Litang line of Ganzi-Litang conjunction zone: Yunnan Geology, v. 3, p. 406–411.
Zhu, Y., Lai, S., Qin, J., Zhang, Z., and Zhang, F., 2019, Late Triassic biotite monzogranite from the western Litang area, Yidun terrane, SW China: petrogenesis and tectonic implications: Acta Geologica Sinica, v. 93, p. 307–321, https://doi.org/10.1111/1755-6724.13758.